EUROPEAN ORGANISATION FOR NUCLEAR RESEARCH

CERN/ISC 98 - 4
ISC/P 35 Add. 2
19 January 1998

ADDENDUM TO THE PROPOSAL P35

COMBINED ELECTRICAL, OPTICAL, AND STRUCTURAL INVESTIGATIONS OF IMPURITIES AND DEFECTS IN WIDE-GAP II-VI COMPOUNDS

CERN[1] - Berlin[2] - Jena[3] - Collaboration

R. Boyn[2], A. Burchard[1], W. Gehlhoff[2], H. Haas[2], F. Henneberger[2], J. Kreissl[2], A. Näser[2], B. Reinhold[2], U. Reislöhner[3], M. Wienecke[2], W. Witthuhn[3], D. Wruck[2]

Spokesperson: M. Wienecke
Contact person: A. Burchard

Geneva 1998

EUROPEAN ORGANISATION FOR NUCLEAR RESEARCH

CERN/ISC 98 - 4
ISC/P 35 Add. 2
19 January 1998

ADDENDUM TO THE PROPOSAL P35

COMBINED ELECTRICAL, OPTICAL, AND STRUCTURAL INVESTIGATIONS OF IMPURITIES AND DEFECTS IN WIDE-GAP II-VI COMPOUNDS

CERN[1] - Berlin[2] - Jena[3] - Collaboration

R. Boyn[2], A. Burchard[1], W. Gehlhoff[2], H. Haas[2], F. Henneberger[2], J. Kreissl[2], A. Näser[2], B. Reinhold[2], U. Reislöhner[3], M. Wienecke[2], W. Witthuhn[3], D. Wruck[2]

Spokesperson: M. Wienecke
Contact person: A. Burchard

SUMMARY

For wide-gap II-VI semiconductors, relatively low doping limits and problems with compensation phenomena are typical. Native defects and residual impurities are found to influence the doping efficiency in a complex manner.
In previous ion implantation experiments performed on ISOLDE we have made considerable progress with the doping problem by using radioactive isotopes of host elements transmuting into relevant dopants (Cd, Te, Se, Sr) and of dopants themselves (Ag, As, In) introduced into CdTe, ZnTe, and ZnSe. Thus we could assign unambiguously defect features in electrical and photoluminescence measurements to extrinsic dopants by means of the half lives of radioactive decay. Under optimum conditions we have found an almost one-to-one doping efficiency relative to the implanted dose.
The experiments proposed now aim i) at the completion of our data on p- and n-type shallow dopants in IIb-VI semiconductors. We will include ii) studies of rare-earth doped IIa-VI systems, in particular SrS/SrZnS doped with Ce, which is the most prospective material for full colour electroluminescence devices. First results on doping by implantation with radioactive isotopes and the observation of the characteristic blue luminescence will be represented.

1. Introduction

Wide-band gap II-VI semiconductor compounds are promising materials for optoelectronics in the visible spectral region. The demand for full colour electroluminescent displays (ELD), short wave length light emitting and laser diodes (LED, LD) motivates the intense research on wide band gap substances, which are the basis to create such devices. The material research in the II-VI field was stimulated at in the beginning of the 90's laser action in the blue range was achieved in diode structures based on ZnSe doped with N [1]. The alkaline earth chalcogenides MgS, SrS (IIa-VI) doped with rare earths as luminescence centres, particularly SrZnS:Ce, are considered to be the most promising materials to achieve intense blue electroluminescence for full colour ELD's [2].

A crucial aspect for the creation of optoelectronic devices is the efficient incorporation of the dopants relevant for the respective application, i) for injection devices as well as ii) for ELD's:
i) The fabrication of LED's and LD's requires to get sufficiently high carrier concentrations by doping with acceptors and donors, which is necessary to achieve satisfactory p-n junctions and metal-semiconductor contacts. For wide-gap semiconductors, however, doping limits and compensation phenomena are typical, the latter arising from (shallow or deep) impurities or native defects of the opposite type. The compensating defects may be present as a consequence of low purity or low perfection of the starting material or may be formed "automatically" parallel to the introduction of the dopant on the desired type of site (self compensation).
ii) Electroluminescence based on optical transitions at deep centres requires the dopant incorporation in well defined valence states and on desired lattice sites. Thus the efficiency of this emission is strongly influenced by impurities and defects, e.g. by the formation of complex centres involving charge transfer effects.

All these phenomena are affected, and in most cases controlled, by the kinds and concentrations of the *intrinsic* defects occurring in the material as a consequence of doping and thermal treatments. Native defects determine the available sites on which the dopants can be incorporated, and, acting as donors or acceptors themselves, take part in the compensation processes described. Additional residual impurities are involved in defect interactions in an similar way.

To investigate the properties of the relevant extrinsic and intrinsic defects, i.e. their electronic and structural features, it is necessary to combine several analysing methods being sensitive to point defects. In our collaboration we combine electrical (Hall effect, C-V, DLTS) optical (photoluminescence spectroscopy, photo-luminescence excitation spectroscopy, transmission spectroscopy) and structural (PAC, EPR) investigations. The basic idea of our experiments is to utilise besides stable dopant elements, radioactive host atoms (or isoelectronic) isotopes, which are incorporated on the corresponding lattice sites, and than transmute into (stable or instable) dopant isotopes. Using the half lives as fingerprints, dopant atoms involved in the relevant centres can be unambiguous identified.
The present addendum is based on the proposal ISC P/35 and the results achieved so far. It is focused on electrical and optical investigations on several II-VI wide gap materials relevant for optoelectronics.

2. Review of current research

The state of international research on II-VI materials related to our experiments can be summarised as follows:
i) Undoped ZnSe can be grown only n type, ZnTe only p type [3]. The introduction of „opposite" types of dopants using common doping techniques leads to unsatisfactory results. The only II-VI compound which can be doped p as well as n type is CdTe, but also in that case the efficiency is limited, mainly by compensation phenomena. The reason lies in the physico-chemically determined self-compensation, but also in the inadequacies of the conventional technologies (e.g. insufficient purity of the starting materials, uncontrolled thermal or implantation damage).
So far, a sufficient p-type conductivity of ZnSe has been achieved only by using the MBE-technology which is distinguished by high purity and low growth temperature [4, 5]. A carrier concentration of up to 10^{18} cm^{-3} being high enough for injection devices can be only realised so far with N doping. Other group V elements are not electrically active, although incorporated substitutionally as revealed by PL spectra [6]. Using group I elements, which also act as acceptors when incorporated on metal lattice sites, the doping limit reached is at only about 10^{16} cm^{-3} [7, 8]. This different dopability in the two sublattices occurs also for n-type doping. Thus the introduction of group VII elements on chalcogen sites leads to higher carrier concentrations (up to 10^{19} cm^{-3} [9]) than In, Al and Ga at metal sites. This reflects the higher stability of the Zn-sublattice and emphasises the importance of site selective doping procedures. An opposite tendency appears for doping ZnTe: for p-type doping up to 10^{20} cm^{-3} [10] N can be electrically active incorporated, whereas on n-type ZnTe little is reported and it is got always only high resistive. Typically, as the dopant concentration is increased above the critical value, the degree of compensation also increases, leading to decrease of the doping efficiency [5, 7, 11].
These phenomena are the subject of the II-VI community's research and several authors discuss various compensation models in connection with native defects and incorporation mechanisms linked with them. Thus, e.g., a N-Se-vacancy complex, coming about with increasing N concentration, has been detected in N-doped ZnSe [11, 12]. In several theoretical works the self compensation is discussed as caused by the dopant impurities „themselves" incorporated on interstitial sites. Reference [13] invokes a thermodynamic equilibrium between Li on metal site and interstitial Li, occurring even at room temperature: donor type interstitial Li compensates Li on metal site acting as an acceptor. In [14] a similar model is discussed also for N doped ZnSe. Interstitial N acting as a compensating shallow donor is incorporated depending on provided lattice sites with increasing N density. For the other group V elements the same author describes, also in a theoretical work, the formation of deep centres for dopants on substitutional sites, due to lattice relaxation resulting in a low symmetry atomic configuration [15]. Such deep As correlated centres where detected by photoluminescence [16]. After [17] the formation of compensating native defects connected with adding shallow dopants in wide-band gap semiconductor compounds is determined by the position of the Fermi level. This model is used in [18] describing the doping limitations that way as in wide gap compounds the Fermi level is pinned in the band gap by localised centres.

These results lead one to the question whether it is possible at all to achieve by means of the common procedures sufficient concentrations of all types of relevant dopants. Which kinds of defects and mechanisms limit the doping efficiencies in a given case? Are there alternative dopants or doping techniques?

Similar questions are relevant for the group IIa-VI compounds and the efficiency of luminescence centres.
ii) It is now generally accepted, that the blue emission of electroluminescent phosphors based on Ce doped SrS is due to two parity allowed 5d - 4f transitions of Ce^{3+} [19]. In the IIa-VI compounds, which have strongly ionic character and very large band gaps, the excess charge of dopants with valences different from the host elements is always compensated by oppositely charged defects, rather than by free carriers (as possible in the semiconductor case). This enables one to increase the concentration of the luminescence centres (and consequently, their efficiency) by introducing „coactivators". Instances exist where the Ce luminescence depends on the presence of Ag^{1+} [21] or K^{1+}, Na^{1+} at cation site and F, Cl anions [22], respectively. Also native defects, such as metal vacancies V_M^{2-} can act as coactivators in IIa-VI compounds [20, 23]. However, it is shown in [24], that post growth annealing treatments of SrZnS:Ce results in an enormous increasing of blue emission due to adjusting the intended valence state of Ce^{3+}.

In our investigations, applying radioactive isotopes, the ion implantation technique is used to add the dopants. This technique has the advantage of high purity achieved by mass separation and controllability of dopant densities. There are very poor systematic investigations on ion implantation of II-VI compounds [25]. For the IIa-VI substance group ion implantation seems to be almost a new field, only recently first results on Ce-ion implantation in SrS were published [26].

3. Previous results of ISOLDE experiment 325

Within the ISOLDE solid state community, so far, investigations of defects produced by radioactive transmutation for II-VI compounds were performed only within the ISOLDE experiment IS 325 using electrical and optical measurements. However, it should be noted that in addition to that work there are many PAC studies referring to donor and acceptor isotopes [27] within the IS 328, which have led to important information on defect structures.

In the previous transmutation experiments we have used the host radioactive isotopes $^{107, 115}$Cd, ^{75}Se, ^{121}Te, and ^{85}Sr transmuting into relevant dopants to dope CdTe, ZnTe, ZnSe by substitutional donors as well as acceptors. Furthermore we used radioactive isotopes of the dopants themselves (^{111}Ag, ^{73}As) to clarify defect features occurring due to doping. First experiments were made using the ^{140}Ba-La-Ce decay to dope SrS with Ce substitutionally.

We have concentrated on electrical and photoluminescence measurements. As an important precondition special investigations were made on the effects and optimisation of the post-implantation annealing. Therefore we performed etching investigations of tracer diffusion and, to avoid the influence of dopants different chemical nature using ^{111m}Cd transmuting into Cd, electrical investigations supplemented by PAC measurements.

The latter results will be presented first.

3. 1. Acceptor and donor dopants

3. 1. 1. Incorporation of implanted Radioactive Isotopes

To obtain the efficiency of any doping technology it is necessary to study the relation between the doping effects (e. g. carrier concentrations) and the concentrations of incorporated dopants. During the post implantation annealing, diffusion occurs and the final chemical density of dopants depends on the diffusion of implanted isotopes into the bulk and on the loss by evaporation from the surface.
In Figs. 1 and 2 this loss is illustrated for metal and chalcogen rich II-VI samples. The number of radioactive isotopes remaining in the samples after different annealing steps was measured by γ-spectroscopy. Depending on the kind of dopants and sample preparation different behaviour is observed. Te-isotopes (Fig.1) are incorporated completely under metal saturated conditions, whereas under chalcogen rich conditions a strong out diffusion occurs (for CdTe above 400°C and for ZnSe above 600°C). For Cd isotopes (Fig. 2) the loss is far less pronounced under chalcogen rich conditions. These results imply that the diffusion mechanisms depend on the non-stoichiometry state of the samples. As we know from earlier investigations [28, 29] metal vacancies are dominant in chalcogen rich CdTe and ZnSe, and in metal rich material the Te- and Se-vacancies, respectively, are the dominant defects. This explains why even for host elements the deviation from stoichiometry determines the incorporated fraction during the annealing process. We have found similar tendencies also for ^{75}Se in ZnSe and ^{83}Rb, which act as shallow acceptors at metal lattice sites in this material[30].

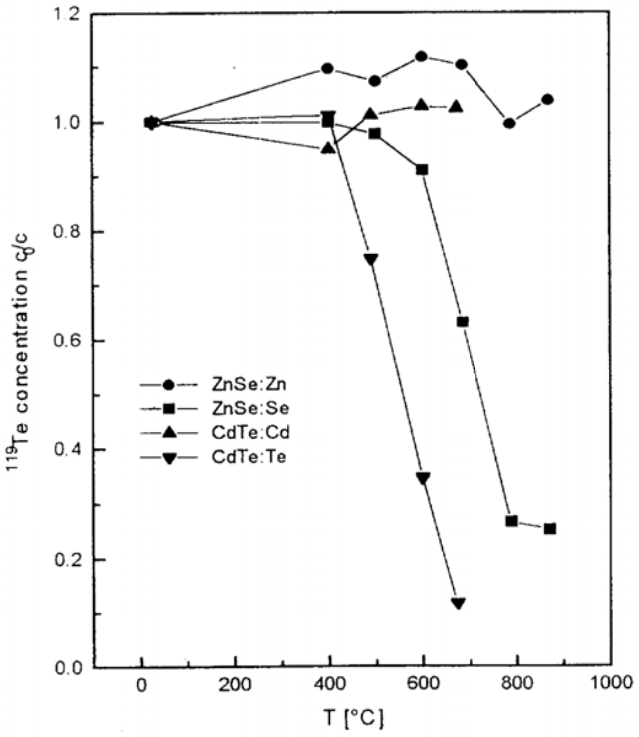

Fig. 1: Fraction of ^{119}Te isotopes remaining in the samples after different annealing temperatures in metal and chalcogen rich CdTe and ZnSe, respectively

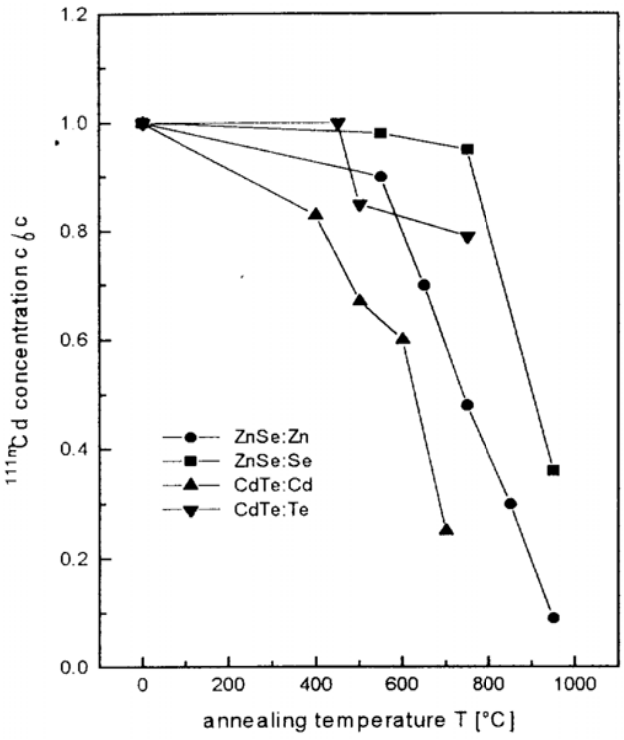

Fig. 2: Fraction of ^{111m}Cd isotopes remaining in the metal and chalcogen rich CdTe and ZnSe samples, respectively, after different annealing steps

Fig. 3 shows concentration profiles of Te in Zn and Se rich ZnSe determined by tracer etching. Obviously different diffusion mechanisms dominate in the two materials as was already indicated by the out diffusion data (Fig. 1). In the Se- rich case, a faster diffusion mechanism occurs, possibly involving interstitial diffusion, because Te diffusion via Zn vacancies is not probable for electronic reasons in this highly ionic compound, and Se-vacancies are not available. In the Zn-rich case a slow diffusion via the dominating Se-vacancies occurs. Analysing the temperature dependence of the Te out diffusion in chalcogen rich samples (compare Fig. 1) reveals an activation energy of E_A = 0.4 eV. This value is much smaller as to be expected for the formation energy of native vacancies in ZnSe. This confirms that vacancies can not be involved in this diffusion mechanism. On the other hand, this fast diffusion does not occur in the Zn-rich case, what is a direct hint to Se vacancies being involved here and shows that these classical diffusion experiments are a useful tool to get information about the native defects in the investigated materials.
The diffusion coefficients calculated from the slope of the ln c = f(x^2) plot (Fig. 3) on the basis of an adequate solution of Fick's second law are in the same order of magnitude as the self diffusion coefficients given in literature [31]. Tracer diffusion investigations with Se isotopes reveal the same tendencies as discussed for Te. Further we investigated in this way the diffusion profiles of As and Rb, whereby the same tendencies as given for the host chalcogen and metal isotopes, respectively, were obtained. These diffusion experiments, particularly the calculated diffusion coefficients depending on non stoichiometry, will be published in detail in [30].

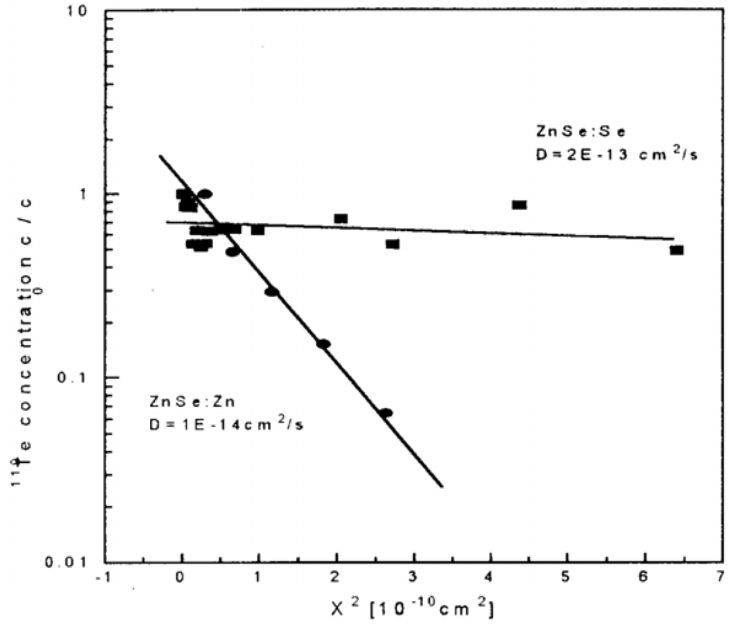

Fig. 3: Diffusion coefficients of Te in ZnSe under Zn or Se saturation at 600°C estimated from concentration profiles determined by tracer etching

A control of diffusion processes is required to adjust doping depths and concentrations as a basis for getting reliable information from other measurements performed in this project, and as basis for applications of such systems. Summarising the discussion above, we have found that Te, Se, and As isotopes are incorporated on chalcogen lattice sites and Cd and Rb occupy sites in the metal sublattice. The knowledge of the diffusion constants can now be used to adjust the concentration and depth distribution by a proper choice of annealing parameters.

In addition to measuring depth profiles and fractions of incorporated atoms, the incorporation of Cd was also studied on the microscopic scale by PAC using the probe atom ^{111m}Cd. Combining nuclear (PAC) and electrical (DLTS, C-V) methods, we have found recently [32] that in CdTe a high fraction of implanted isotopes is incorporated at undisturbed cubic lattice sites even without annealing, and that the disturbed fraction disappears after firing the samples above 400°C. PAC results for CdTe, ZnTe and ZnSe are given in Table 1.

	annealing temperature	fraction	band gap
CdTe	as implanted above 400°C	38% 100%	1.5 eV
ZnTe	above 600°C	100%	2.4 eV
ZnSe	at 550°C at 950°C	60% 70%	2.7 eV

Table 1 PAC results on the incorporation of Cd: fraction of ^{111m}Cd atoms with no detectable anisotropic hyperfine interaction, i.e. on sites with cubic symmetry

For ZnTe having a middle bandgap compared with CdTe and ZnSe a 100% annealing, e. g. 100% cubic environment of implants occurs above 600°C. For ZnSe an undisturbed fraction of only 60% is found after annealing at 550°C. A complete annealing of implantation damage doesn´t appear even after firing at 950°C. That indicates a relation between damage annealing and lattice binding energies, i. e. formation energies of native defects.
Nevertheless, even in ZnSe at least a majority of 70% of the implanted Cd is incorporated defect-free, whereas the incorporation is perfect in the other compounds.

3. 1. 2. Electrical measurements on samples doped with Radioactive Isotopes

The preceding section demonstrated how implanted host or isoelectronic elements can be incorporated efficiently at the respective lattice sites and that implantation defects can be minimised. This result is the basis of the following transmutation doping experiments, where host elements are implanted which then transmute into relevant dopants at room temperature.

Fig. 4 shows C-V profiles in Te rich CdTe implanted with ^{107}Cd isotopes transmuting into Ag with a half life of 6.5h. In the bulk of the sample, i.e. in a depth about 1 µm, the pre annealed carrier concentration of $p = 10^{16}$ cm^{-3} is nearly reproduced. The slight decrease towards the surface is a hint for the existence of some residual defects. During the transmutation the doping density at smaller depths drastically increases. The size and shape of this profile corresponds to the profile expected by implantation and diffusion: the carrier profile can be described by a gaussian distribution with a maximum at 10^{17} cm^{-3} and a half width corresponding to the diffusion length as calculated from the self diffusion coefficients [31]. The Ag isotopes transmuting from the incorporated substitutional Cd act as acceptors with an efficiency of 100%. Obviously the transmutation occurs without any detectable compensation and distortion of local structure by any recoil. The doping effect of Ag is also confirmed by the time dependence of the reverse bias at fixed capacitance, which is a measure for the carrier concentration [33, 34]. It increases exactly with the expected half life as shown in Fig. 5.

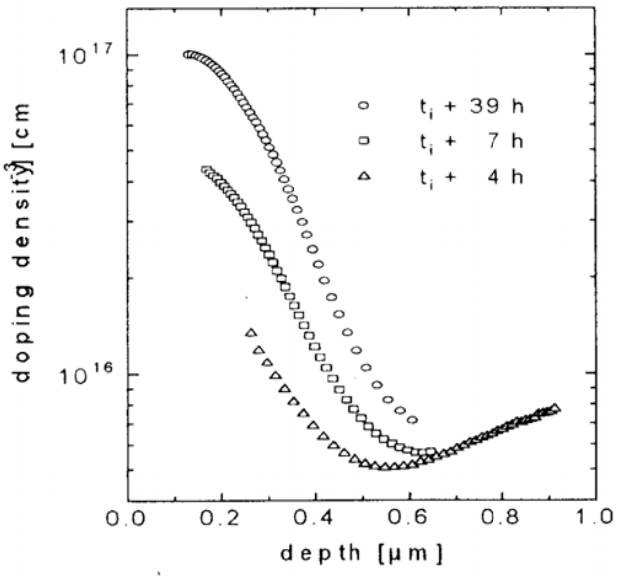

Fig. 4:Additional doping in p-CdTe by transmutation of ^{107}Cd into Ag measured with differential C-V-technique at various times after implantation,
t_i - implantation time

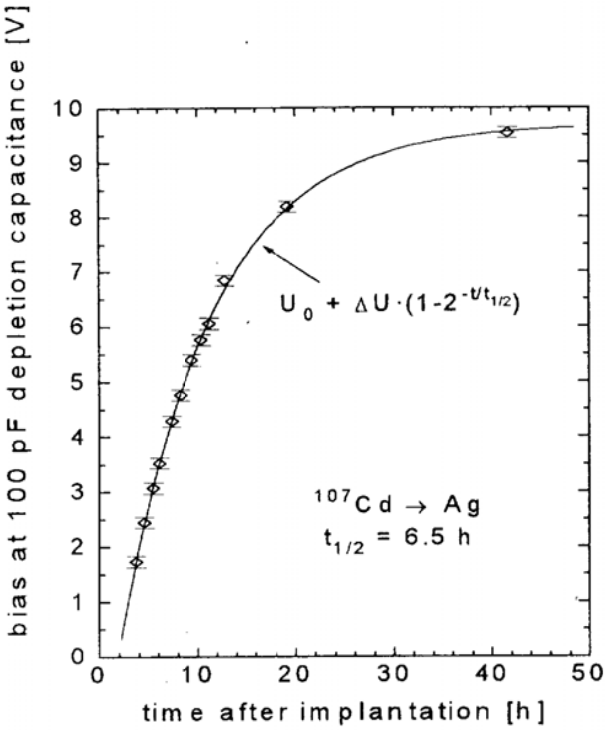

Fig. 5: Increasing doping in p-CdTe by transmutation of ^{107}Cd into Ag detected by the time-dependent bias at a fixed capacitance (see Fig. 4)

A similar effect was found also in ZnTe doped with In by transmutation of radioactive ^{115}Cd (Fig. 6). Here the In donors compensate the p-type conductivity in bulk ZnTe and the voltage at the contact decreases. As both the metastable and the ground state of the ^{115}Cd isotope had been implanted, the observed time dependence is a superposition of two exponential functions reflecting the half life of these ^{115m}Cd and ^{115g}Cd states. Related from the values of ΔU_g to ΔU_m (Fig. 6), we found the ratio of the isotope states to be 5 :7.

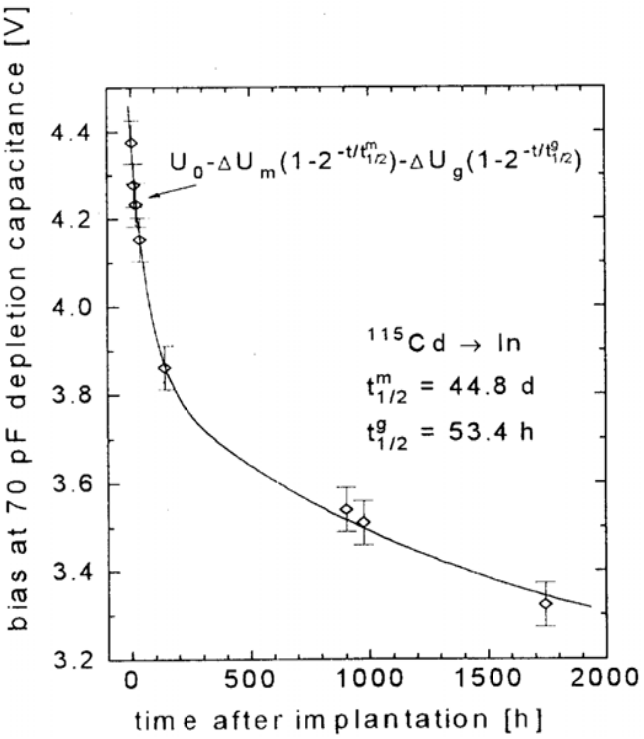

Fig. 6: Time-dependent compensation in p-ZnTe by transmutation of ^{115}Cd into In showing both the half-lifes of groundstate (g) and metastable (m) isotopes.

Transmutation experiments were also performed on ZnSe, concentrating on acceptor dopants that do not form effective acceptors in conventional doping experiments. Fig. 7 shows the time dependence of the sheet resistivity of a ZnSe sample implanted with ^{107}Cd transmuting into Ag. The decreasing conductivity with exactly the half live of the radioactive decay (6.5h) is interpreted as caused by Ag acceptors compensating the n-type ZnSe. Finally the sample became highly resistive.

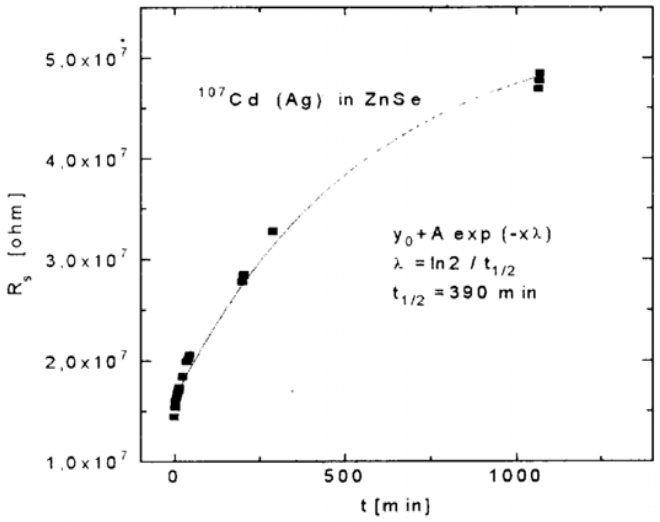

Fig. 7: Increasing sheet resistivity in n-type ZnSe by transmutation of ^{107}Cd into Ag detected by time dependent conductivity measurements

A change in conductivity type was not observed. P-type conductivity was achieved after implantation of ^{75}Se decay to As and ^{85}Sr decay to Rb in very pure [29] vapour grown ZnSe samples. Table 2 summarises the measured conductivities and carrier concentrations.

dopant	fluency [cm^{-2}]	depth [µm]	T_{anneal} [°C]	σ [Ω^{-1} cm^{-1}]	p [cm^{-3}]	µ [cm^2/Vs]	doping efficiency [%]
^{75}Se(As)	2 E11	1	920	4 E-2	2 E15	90	100
^{85}Sr(Rb)	1 E10	0.6	600	2 E-5	5 E13	3	30

Table 2 Transmutation doping results in ZnSe as measured by the Van der Pauw method (σ- conductivity, p - carrier concentration, µ - mobility, efficiency - ratio of carrier concentration to fluency/depth)

The hole concentrations (p) achieved are relatively small due to the low yields available for those special radioactive ion beams. Nevertheless, taking into account the limited accuracy of the van der Pauw measurements these experiments reveal that As and Rb act as efficient acceptors in ZnSe. This has been concluded from photoluminescence investigations in the literature [16] but has not been demonstrated by electrical measurements until now. The results concerning the electrical measurements are published in [33, 34].

3. 1. 3. Photoluminescence measurements on samples doped with Radioactive Isotopes

To demonstrate the transmutation effects also in photoluminescence, in particular for ZnSe, was our main goal in the last experimental period. The main problems encountered in these experiments were: i) in ZnSe the implantation damage can be removed to a large extent but not completely, and the residual defects reduce light emission from the implanted region, ii) residual impurities present in ZnSe with concentrations of some 10^{16} cm^{-3} and even much higher Zn-vacancy density dominate the PL-spectra [29], iii) the region investigated by PL is much deeper than the original doped layer. The diffusion study as performed in 1996 allowed us to optimise the post-implantation annealing to get diffusion profiles required for successful PL-measurements. Such measurements were made by us in the 1997 period.

Fig. 8 shows PL-spectra of ZnSe implanted with $^{85}Sr(Rb)$ at several times after implantation. Unambiguously an acceptor bound exciton (A^0,X) at 2.7927 eV can be correlated to the Rb acceptors formed by radioactive decay from ^{85}Sr, which was incorporated as isoelectronic element on metal lattice sites. The intensity of this line normalised to the intensity of the 1LO phonon replica of the free exciton is plotted as function of time in Fig. 9. Obviously, this intensity ratio, as a measure for dopant concentration, changes in time with the expected half life.

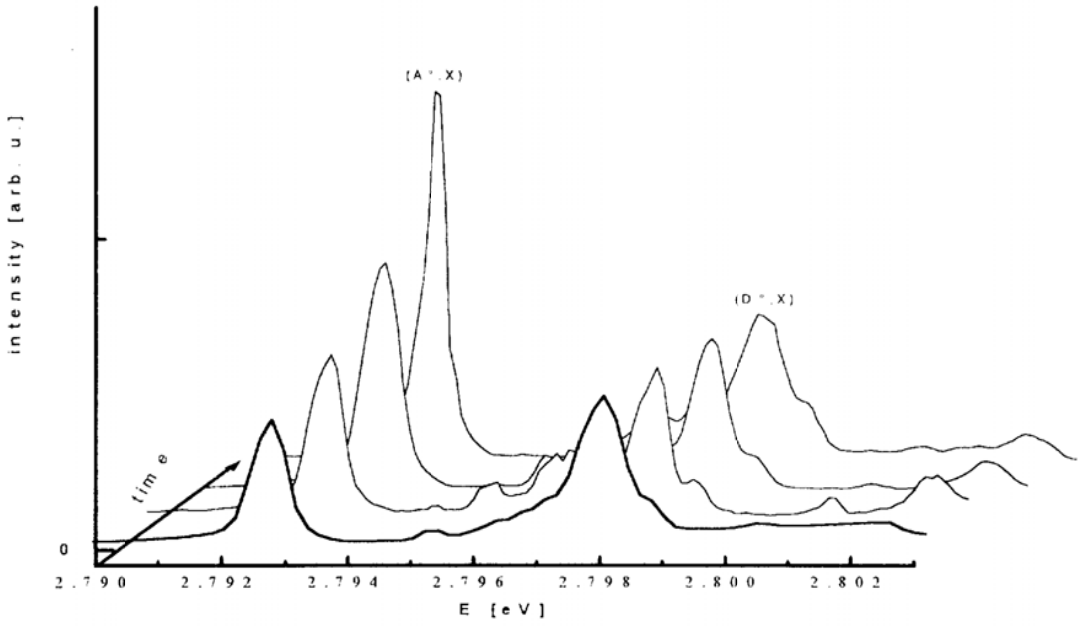

Fig. 8: Photoluminescence spectra of a ^{85}Sr implanted sample, ^{85}Sr decays into Rb ($t_{1/2}$ = 64,8 d)

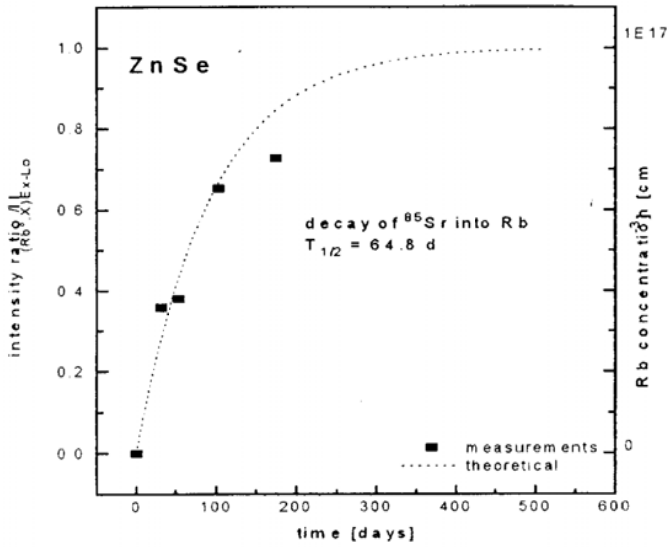

Fig. 9: Normalised intensity of the A^0,X line at 2,7928 eV (see Fig. 8) versus time

Particularly the experiments done with ^{73}As in ZnSe turned out to be very instructive characterising the compensation process: For these experiments we implanted ^{73}Se but annealed the samples only when most isotopes had been transmuted into As. Thus these experiments are comparable to our investigations performed with stable As, revealing always two defect features: a week (A^0,X) line at 2,793 eV, which disappears after further annealing steps, and a broad intense luminescence band at 2,16 eV correlated to a doping induced deep center, similar to a defect feature also found by [16]. Both features we also found in the samples doped with radioactive As, as expected.

As shown in Fig. 10, the time dependence of the A^0,X line (also normalised) can be well fitted with the half live of ^{73}As decaying to Ge, which leads us to assign this line to centres containing As.

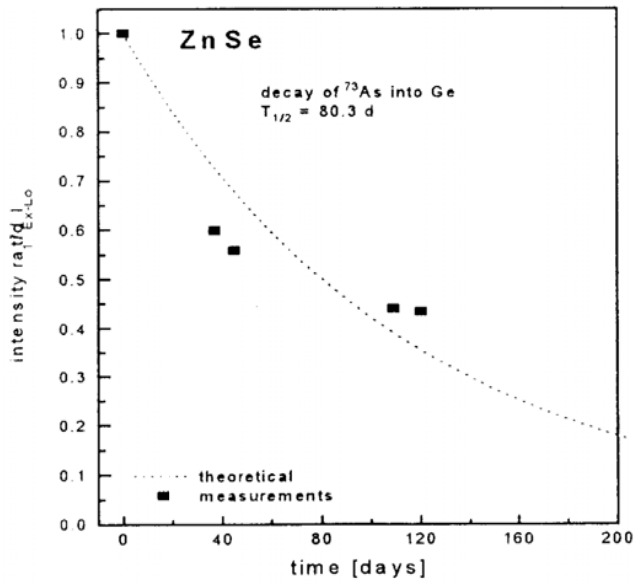

Fig. 10: Normalised intensity of the A^0,X line at 2,7931 eV (see text) versus time

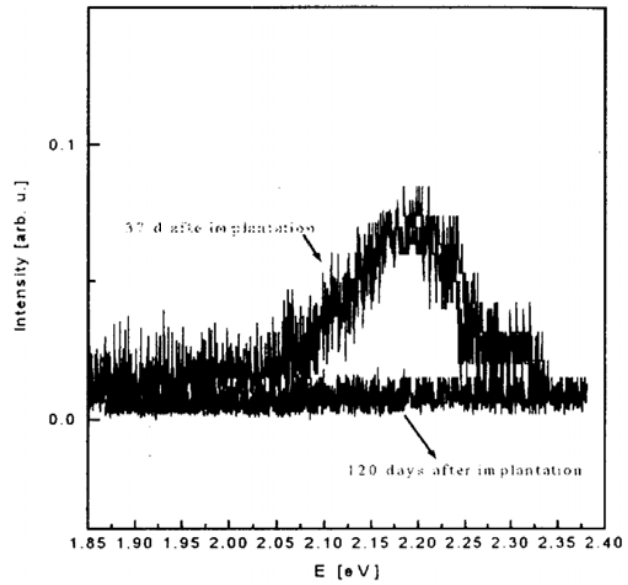

Fig. 11: Deep level in ZnSe after As implantation, annealed at 600°C, for comparison the same sample after some half lives is shown being identical to an undoped reference

Fig. 11 represents the broad emission band of a sample short time after implantation and the same spectral region after some half lives, for comparison a spectrum of an undoped sample is added. The emission vanishes completely, indicating, that the origin of this deep centre is the dopant As too, and not, however, a thermal or implantation damage.

To complete our investigations on Ag doped CdTe made so far by electrical measurements [33, 35], the transmutation $^{111}Ag \rightarrow Cd$ was investigated in CdTe by photoluminescence measurements, too. Here the Ag correlated acceptor bound exciton disappears according the expected half life (Fig. 12). This confirms the role of Ag, being always present in CdTe with concentrations up to 10^{16} cm^{-3}, as an efficient shallow acceptor.

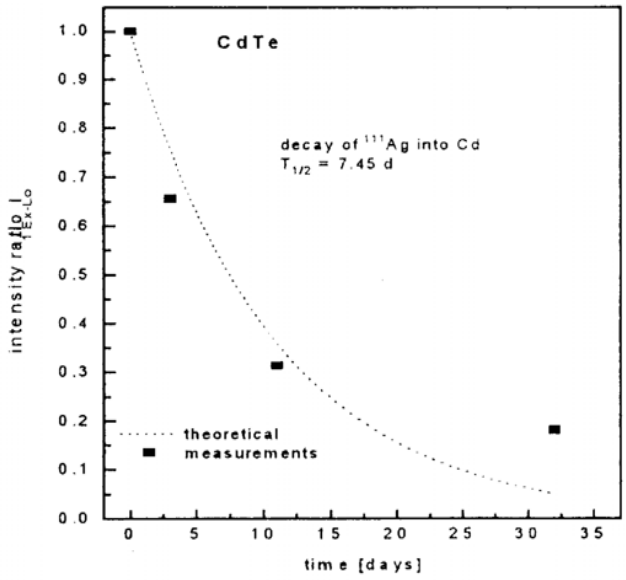

Fig. 12: Normalised intensity of the Ag correlated acceptor bound exciton versus time

3. 2. Preliminary studies of alkaline-earth chalcogenides with rare earth dopants (SrS:Ce)

Our systematic investigations will be extended to IIa-VI materials doped with rare earths. Here we present the first results we obtained in this field.
Polycrystalline thin film SrS samples grown by MBE technology on Si were implanted with a 10^{14} cm^{-2} dose of ^{140}Cs ($t_{1/2}$ = 65s) which transmutes over Ba ($t_{1/2}^1$ = 12.79d) and La($t_{1/2}^2$ = 40.3h) into Ce (for this kind of luminescence minimum dopant densities of 10^{18} cm^{-3} are necessary). They have been annealed for the first time after 12 days, when about half of the maximum Ce concentration has emerged. After that they show an impressive blue luminescence at 474 nm (Fig. 13). With ongoing time the intensity of this blue band decreases.

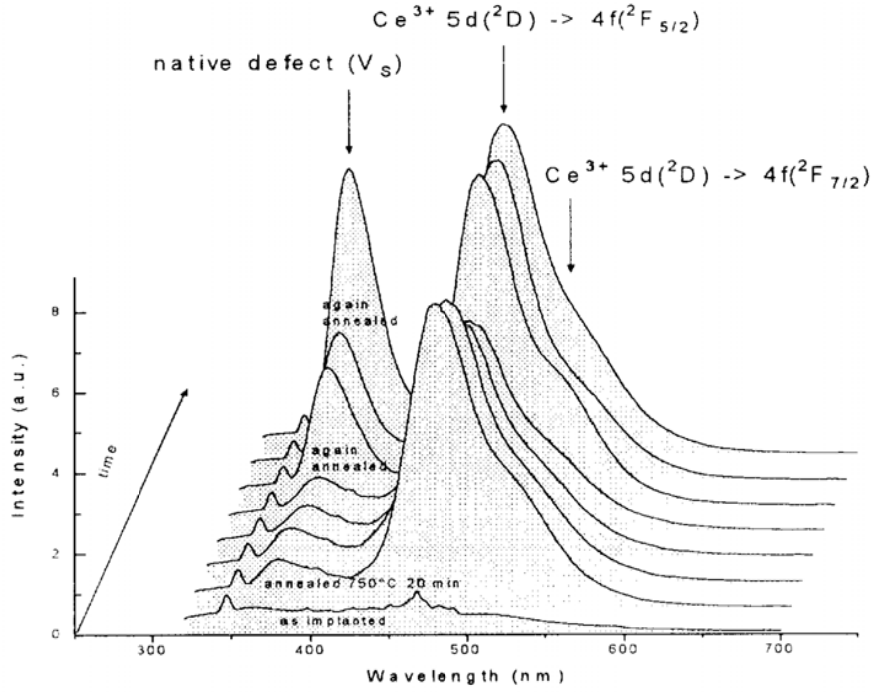

Fig. 13: Emission spectroscopy on SrS implanted with ^{140}Cs ($\rightarrow$Ba$\rightarrow$La)$\rightarrow$Ce

The mechanism causing this behaviour is unclear. Since this change follows $t_{1/2}^1$ (Fig. 14) there might be a correlation with the transmutation process ($t_{1/2}^1 >> t_{1/2}^2$). On the one hand the calculated recoil energies are smaller than the displacement energies (about 10 eV in SrS [20]) and a transmutation on lattice sites should be expected. On the other hand, the decay takes place via β^- emission, which may produce damage itself or may lead to a charge state of the emerging Ce centres different from 3+. Both processes may contribute to the decrease of the efficiency of the blue emission.

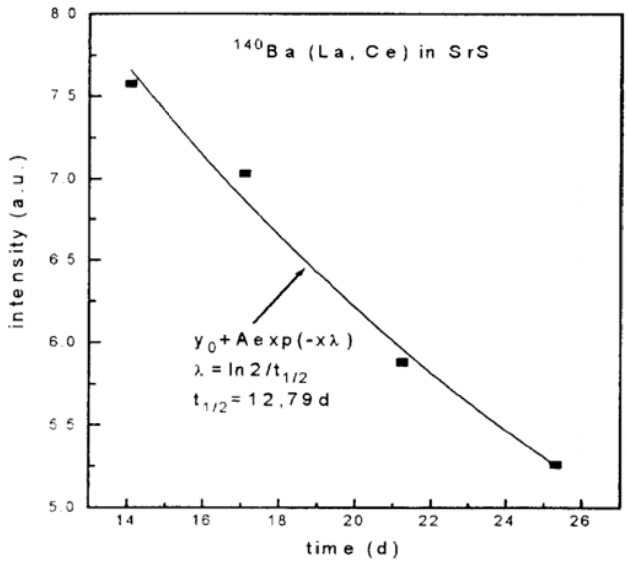

Fig 14: Time dependent intensity of the 474 nm luminescence band after implantation and the first annealing step at 750°C (see Fig. 13)

As shown in Fig. 13 after further annealing steps the intensity of the 474 nm band increases again according to the increasing concentration of the Ce isotopes transmuted in the meantime from the Ba. As shown in Fig. 15, the time dependence of the increasing intensity after the several steps is consistent with the expected half live. This can be interpreted as an hint therefore that the 3+ valance state which is necessary for the blue luminescence is to be thermally activated.

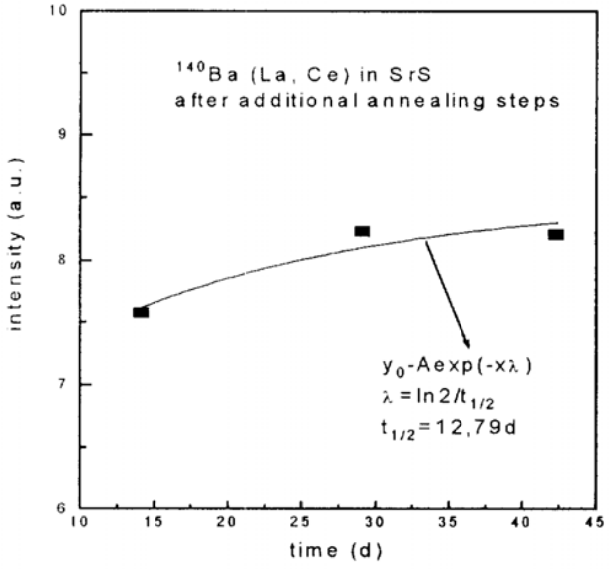

Fig. 15: Intensity of the 474 nm luminescence immediately after further annealing steps versus time after implantation

The emission spectra (Fig. 13) further show, a band at 380 nm stimulated by the annealing treatments. This band also occurs in the not implanted area of the samples and its change in intensity cannot be described by the transmutation times. This band has been also observed in SrS:Ce in [23] and has been assigned to S vacancies.

These preliminary results confirm that charge compensation phenomena and effects of native disorder are important also for the efficiency of the systems considered here. systematic studies as planned by us should contribute to the optimisation of such materials.

4. Proposed Experiments

In the experiments to be performed we intend i) to complete the study on shallow donors and acceptors in II-VI semiconductors and ii) to extend the investigations on rare earth luminescence centres in IIa-VI compounds. The isotopes to be used were chosen mainly on the basis of the following:

- # The elements selected for implantation should be isoelectronic to the host elements, and the respective decay products should act as shallow dopants or luminescence centres, respectively , if incorporated on *substitutional* sites.
- # Convenient magnitudes of the half lives for the relevant decay processes.
- # Recoil energies smaller than the respective host displacement energies.
- # Availability of beam intensities sufficient for obtaining the doping concentrations which are required for the measurements to be performed (section 2).
- # We have included dopants having isotopes which can be used as PAC probes, in order to enable the electrical and optical results to be correlated with PAC measurements in the ISOLDE experiment IS328, and, if possible, to perform common beam times with other PAC groups.

In the following we list the relevant transmutation reactions together with the problems to be studied in each case:

$^{73}\mathrm{Se} \xrightarrow[\text{in ZnSe}]{7{,}1\mathrm{h}} {}^{73}\mathrm{As} \xrightarrow{80{,}3\mathrm{d}} \mathrm{Ge}$ # incorporation of the dopant As for characterising the deep compensating centre detected already optically (see previous results) by DLTS

$^{75}\mathrm{Se} \xrightarrow[\text{in ZnSe}]{118{,}5\mathrm{d}} \mathrm{As}$ # preparation of samples for transmutation doping, performing time dependent Hall effect measurements, aiming at higher doping levels as reached before (see previous results)

$^{83}\mathrm{Sr} \xrightarrow[\text{in ZnSe}]{32{,}4\mathrm{h}} {}^{83}\mathrm{Rb} \xrightarrow{86{,}2\mathrm{d}} \mathrm{Kr}$ # incorporation of the dopant Rb, characterising compensation phenomena by PL to optimise doping of ZnSe with (stable) Rb

$^{85}Sr \xrightarrow[\text{in ZnSe}]{64,8d} Rb$

preparation of samples for transmutation doping, performing time dependent Hall effect measurements, aiming at higher doping levels as reached before (see previous results)

$^{140}Ba \xrightarrow[\text{in SrS}]{12,79d} {}^{140}La \xrightarrow{40,3h} Ce$

incorporation of (Ba) Ce at metal lattice sites, investigation of luminescence mechanisms and efficiencies

$^{141}Ce \xrightarrow[\text{in SrS}]{32,5d} Pr$

incorporation of Ce centres by direct ion implantation, sites of incorporation and luminescence efficiency different from previous case?

$^{111}Ag \xrightarrow[\text{in SrS}]{7,5d} Cd$

incorporation of Ag as co activator in Ce doped samples (ion implantation of stabile Ce, growth), investigations on effects on Ce luminescence

Well defined concentrations of intrinsic defects (including well defined deviations from stoichiometry) in the samples will be established by performing heat treatments, before and after implantation, under group II and group VI rich conditions. The post-implantation treatments aim, in particular, at the annealing of radiation damage and a controlled diffusion of dopants.

5. Experimental Requirements

The proposed experiments can be performed at the General Purpose Separator (GPS). The required isotopes can be produced by standard targets and ion sources. These ion beams can be shared with other users, especially with the experiments IS 328, IS 321, IS 318, and IS 330. Because of the peculiarities of the doping experiments, we need relatively high ion fluences up to 10^{12} cm^{-2}, that means minimum yields of 10^8 to 10^9 s^{-1} to limit the implantation duration to about 1 h.

We want to use the existing infrastructure, i. e. the solid state physics implantation chamber, the High Voltage Platform, and the common solid state physics laboratory. The necessity of using the High Voltage Platform results from preliminary experiments carried out with stable isotopes on the 350 keV accelerator of the Humboldt University. These experiments showed that, particularly for successful photoluminescence measurements, an implantation depth as large as realised by ionic energies of this magnitude is necessary.

For carrying out chemical and contact preparations and annealing we need relatively much space in the solid state physics laboratory, which we could share with other

users. For electrical measurements and g-spectroscopy we need up to 10 m^2 in the ISOLDE hall or in another users' room.
No additional requests are made to the CERN ISOLDE separator group.

7. Beam time Request

Beam	Min. intensity	Target material	Ion source	Shifts
^{73}As ^{75}Se	1E09	Nb foil	Hot plasma	2
^{85}Sr ^{83}Rb	1E09	Nb foil	W-surface	2
^{111m}Ag ^{117}Ag	8.12E08	UC2	Laser ion source	4
^{141}Ba ^{141}Ba	4.5E09	UC2	W-surface	4
			Σ	12

Literature

[1] R.M. Park, M.B. Trofer, C.M. Rouleau, J.M. De Puydt, M.A. Haase, Appl. Phys. Lett. **57** (1990) 2127.

[2] P. J. Soininen, E. Nykänen, L. Niinistö and M. Leskelä, Inorganic and Organic Electroluminescence, ds. R. H. Mauch and G.-H. Gumlich, (Wissenschaft und Technik Verlag, Berlin, 1996) 149-151

[3] H. Hartmann, R. Mach, B. Selle, in: Current Topics in Material Science, vol. 9, North Hollans Publishing Company, Amsterdam, 1982

[4] J. Qui, J. M. DePuydt, H. Chung, M. A. Haase, Appl. Phys. Lett. **59** (1991) 2993

[5] Z. Yang, K. A. Bowers, J. Ren, Y. Lansari, J. W. Cook, J. F. Schetzina, Appl. Phys. Lett. **61**, 22 (1992) 2671

[6] E. Tournié, C. Morhain, C. Ongaretto, V. Bousquet, P. Brunet, G. Neu, J.-P. Faurie, R. Triboulet, J. O. Ndap, Mater. Sci. Eng. B**43** (1997) 21

[7] K. Ohkawa, A. Tsujimura, S. Hayashi, S. Yoshii, T. Mitsuyu, Physica B **185** (1993) 112

[8] Z. Zhu, H. Mori, T. Yao, J. Appl. Phys **73**, 3 (1993) 1146

[9] K. Ohkawa, T. Mitsuyu, O. Yamazaki, J. Appl. Phys. **62**, 8 (1987) 3216

[10] J. F. Swenberg, M. W. Wang, R. J. Miles, M. C. Phillips, A. T. Hunter, J. O. McCaldin, T. C. McGill, J. Cryst. Growth **138** (1994) 692

[11] I. S. Hauksson, J. Simpson, S. Y. Wang, K. A. Prior, B. C. Cavenett, Appl. Phys. Lett. **61** (1992) 2671

[12] T. Yao, T. Matsumoto, S. Sasaki, C. K. Chung, Z. Zhu, F. Nishiyama, J. Cryst. Growth, **138** (1994) 290

[13] G. F. Neumark, J. Appl. Phys. **51** (19980) 3383

[14] D.J. Chadi, J. Cryst. Growth **138** (1994) 925

[15] D. J. Chadi, Appl. Phys. Lett. **59** (27) (1991) 3589

[16] Y. Zhang, B. J. Skromme, S. M. Shibli, C. Tamargo, Phys. Rev. B **48** (15) (1993) 10885

[17] G. Mandel, Phys. Rev. **134** (1964) A1073

[18] W. Faschinger, S. Ferreira, H. Sitter, R. Krump, G. Brunthaler, Materials Science Forum **182-184** (1995) 29

[19] S. Yokone, T. Abe, T. Hoshina,
J. Phys. Soc. Japan **46** (1979) 351

[20] P. K. Ghosh, B. Ray, Prog. Crystal Growth and Charact., vol. 25 (1992) 1

[21] K. O. Velthaus, B. Hüttl, U. Troppenz, R. H. Mauch, 1997 SID Internat. Symp., Digest of Technical Papers, pp. 411-414

[22] W.-M. Li, M. Ritala, M. Leskelä, R. Lappalainen, M. Karjalainen, E. Soininen, C. Barthou, P. Benalloul, J. Benoit, E. Nykänen, L. Niinistö, Extended Abstracts of Intern. Conf. on Science and Technology of Display Phosphors, Huntington Beach, California, Nov. 1997, p. 109

[23] Ravinda Pandey, S. Sivaraman, J. Phys. chem. Solids **52**, 1 (1991) 211

[24] Sang Tae Lee, M. Kitagawa, K. Ichino, H. Kobayashi,
Applied Surface Science, **100/101** (1996) 656

[25] V. X. Quang, B. Selle, "Ionenimplantation in II-VI-Verbindungen", Akademie der Wissenschaften der DDR, Zentralinstitut für Elektronenphysik, Preprint 88-3, Aug. 1988

[26] W.-M. Li, R. Lappalainen, J. Jokinen, M. Ritala, M. Leskelä, E. Soininen, Extended Abstracts of Intern. Conf. on Science and Technology of Display Phosphors, San Diego, California, Nov. 1996, p. 135

[27] Th. Wichert, Th. Krings, H. Wolf, Physica B **185** (1993) 297

[28] M. Wienecke, H. Berger, M. Schenk, Mater. Sci. Eng. B **16** (1993) 219

[29] M. Wienecke, B. Reinhold, G. Gorbunova, V. Kasiyan,
Mater. Sci. Eng. B **43** (1997) 112

[30] M. Wienecke, B. Reinhold, S. Hermann and the ISOLDE Collaboration, sumitted to X. ICCG Jerusalem, Israel, to be published in J. Cryst. Growth

[31] D. Shaw, J. Cryst. Growth **86** (1988) 778

[32] N. Achtziger, J. Bollmann, Th. Licht, B. Reinhold, U. Reislöhner, J. Röhrich, M. Rüb, M. Wienecke, W. Witthuhn, ISOLDE collaboration,
Semicond. Sci. Technol. **11** (1996) 947

[33] M. Wienecke,J. Bollmann, J. Röhrich, K. Maass, B. Reinhold, D. Forkel-Wirth, J. Crystal Growth, **161** (1996) 82

[34] M. Wienecke, B. Reinhold, J. Röhrich, J. Bollmann, N. Achtziger, U. Reislöhner, W. Witthuhn, S. Hermann, submitted to be published in J. Appl. Phys. 1998

[35] J. Bollmann, M. Wienecke, J. Röhrich, H. Kerkow,
J. Crystal Growth, **159** (1996) 384